ELSEVIER

Biochimica et Biophysica Acta 1459 (2000) 69–76

BIOCHIMICA ET BIOPHYSICA ACTA
BBA

www.elsevier.com/locate/bba

The natural product capsaicin inhibits photosynthetic electron transport at the reducing side of photosystem II and purple bacterial reaction center: structural details of capsaicin binding

A. Spyridaki [a,b], G. Fritzsch [b], E. Kouimtzoglou [a], L. Baciou [c], D. Ghanotakis [a,*]

[a] *Department of Chemistry, University of Crete, 71409 Heraklion, Crete, Greece*
[b] *Max-Planck-Institute of Biophysics, Heinrich-Hoffman-Str. 7, Frankfurt, Germany*
[c] *CGM, Bat. 24, CNRS, 91198 Gif-sur-Yvette, France*

Received 30 November 1999; received in revised form 7 March 2000; accepted 15 March 2000

Abstract

Capsaicin, a natural quinone analog, was found to block electron transport, in both plant photosystem II (PSII) and bacterial reaction center (RC) from *Rhodobacter sphaeroides*, at the Q_B site. The mode of action of capsaicin was investigated by O_2 evolution measurements and fluoresence induction studies in the case of PSII, and flash-induced absorbance spectroscopy in the case of the bacterial RC. Structural details of capsaicin binding to the bacterial RC complex were determined by X-ray crystallographic analysis.

Keywords: Photosystem II; Purple bacteria; Capsaicin; Herbicide; X-ray structure

1. Introduction

The photosynthetic reaction centers (RCs) of PSII and of purple bacteria share many common features, especially at the acceptor side [1]. One common characteristic is the capability of the secondary quinone (Q_B) binding site to accommodate a variety of structurally different substances [2–4]. These substances include herbicides, which are widely used in agriculture. They belong to several chemical classes: urea, triazines, uraciles, phenols and cyanoacrylates. A common mechanism has been proposed for inhibition: displacement of Q_B from its binding site. All the inhibitors bind to the same pocket of the protein, although they occupy overlapping, but not identical, regions.

Recently, the structure of the RC from *Rhodobacter sphaeroides* was refined up to 2.2 Å resolution and the Q_B-binding pocket was well defined [5–7]. In purple bacterial RCs, the herbicide binding site is located on the L subunit in the connecting loop between the fourth (D) and the fifth (E) transmembrane helices. The high resolution crystal structures of the RCs from the photosynthetic bacteria *Rhodopseudomonas viridis* and *Rb. sphaeroides* have been used as templates for the construction of three-dimensional models for a number of PSII RC subunits including the herbicide-binding niche [8–12]. In analogy to the bacterial RC, it is assumed that the Q_B-

Abbreviations: Capsaicin, 8-methyl-vanillyl-6-nonenamide, MVNA; DCMU, 3-(3,4-dichlorophenyl)-1,1-dimethylurea; DCBQ, 2,6-dichloro-benzoquinone; LDAO, *N*,*N*-dimethyldodecylamine *N*-oxide; PSII, photosystem II; RC, reaction center

* Corresponding author.;
E-mail: Ghanotakis@chemistry.uch.gr

0005-2728/00/$ – see front matter
PII: S0005-2728(00)00114-6

binding site in PSII is composed exclusively of D1 protein residues corresponding to those in the Q_B pocket of the L protein in the 1PRC structure [13] and in a similar position relative to the quinone coordinates [14]. Structural analyses of the Q_B-binding site in *Rp. viridis* and *Rb. sphaeroides* RCs have confirmed the existence of a 'distal' and a 'proximal' position of the Q_B head group, where the former is located about 5 Å further away from the non-heme iron than the latter [5,15,16]. In *Rb. sphaeroides* RC, the distal position was found in dark adapted RCs. A hydrogen bond is formed between the peptide nitrogen of Ile L224 and the Q_B head group. The proximal position has been observed in light-induced (charge-separated) RCs. In this position, a hydrogen bond between His L190 and Q_B, which connects the quinone to the direct pathway of electron transfer from $Q_A^- Q_B$ to $Q_A Q_B^-$, is observed. Despite significant sequence homologies between the Q_B-binding pocket of purple bacteria and PSII, herbicides of the urea-type and phenol-type do not or only moderately act as inhibitors of electron transport in the bacterial reaction center. The only exceptions are the *s*-triazine herbicides and 2-iodo-4-nitro-6-isobutylphenol.

Capsaicin (8-methyl-vanillyl-6-nonenamide, MVNA) is the pungent principal component of red pepper species (capsicum species). It is composed of three major functional moieties, namely, a vanilloid, an amide and a hydrophobic side chain, having characteristics of both phenol and urea/triazine type PSII inhibitors. This compound has been reported to act as a competitive inhibitor for ubiquinone in NADH-ubiquinone oxidoreductase isolated from several organisms [17–21]. In the present communication, we report that capsaicin can act as an inhibitor at the Q_B site in the photosynthetic reaction center of purple bacteria and plants. Structural details of capsaicin binding to the bacterial RC complex were determined by X-ray crystallographic analysis.

2. Materials and methods

2.1. Biological materials

PSII membranes were prepared from spinach as described in [22].

The preparation of the RC from *Rb. sphaeroides* was performed as described in [23]. The RC was crystallized in the Q_B-depleted form. Removal of Q_B was achieved as described in [16].

2.2. Analytical procedures

Capsaicin-induced inhibitory activity on PSII was measured at pH 7 by O_2 evolution rates in the presence of DCBQ as an electron acceptor with a Clark-type oxygen electrode.

Fluorescence induction kinetic measurements at room temperature were performed with the portable instrument plant efficiency analyzer (PEA) built by Hansatech Instruments.

The recombination decay kinetics detected at 865 nm after a laser saturating actinic flash were measured by a home-made single-beam spectrophotometer. At this wavelength, the reduction of the oxidized primary donor (P^+) is followed. In the absence of an inhibitor the charge recombination is due to $P^+ Q_{B^-} \rightarrow P Q_B$, while in the presence of the inhibitor to $P^+ Q_A^- \rightarrow P Q_A$. The exponential decompositions of the charge recombination kinetics were achieved with a home-made program using a Marquard algorithm. The fraction of the reaction centers with bound Q_B has been determined as $f_{Q_B} = A_2/(A_1 + A_2)$, where A_1 is the amplitude corresponding to the recombination from Q_A (rate constant is 10 s^{-1}) and A_2 is the amplitude corresponding to recombination from Q_B (rate constant is 1 s^{-1}). Inhibition titrations were carried out in the presence of external ubiquinone-6 (UQ6) in order to obtain 50% Q_B activity. Small aliquots of capsaicin, dissolved in ethanol, were added.

2.3. Crystallization

Crystallization was performed by vapor diffusion at 21°C. The protein droplets contained 0.1% (w/v) LDAO, 3% (v/v) 1,4-dioxan, 3% (w/v) 1,2,3-heptanetriol, 1% (w/v) 1,2,3-hexanetriol and 0.7 M potassium phosphate (pH 7) as a precipitant. This mother liquor was equilibrated against a reservoir solution containing 1.5 M potassium phosphate. Crystals, which appeared after 2 weeks, were soaked with 2.6 mM capsaicin for 3 days.

The crystals obtained belong to the trigonal space

group $P3_121$ with unit cell dimensions of 141.50 Å, 141.50 Å, 187.15 Å, 90°, 90°, 120°.

2.4. Structure determination and refinement

Diffraction data were collected at room temperature from a single crystal using monochromatic synchrotron radiation at a wavelength of 1.3 Å of beamline BW6 from the Max-Planck Research Unit at DESY (Hamburg). The oscillation images were processed with the program packages DENZO and SCALEPACK [24,25]. The wild-type structure [7] was used as a starting model for the approximation of initial phases and the construction of an initial model. The initial coordinates for capsaicin were obtained using the SYBYL molecular modeling package. Topology and parameter files for capsaicin were generated by XPLO2D [26–28].

Crystallographic refinement was performed using iterative cycles of simulated annealing, combined with the energy minimization option and restrained individual B-factor refinement with the program CNS. Manual inspection and refitting were performed with the molecular graphics program O [29]. After each round of refinement, the geometry was checked with the program package PROCHECK [30,31]. The coordinate error was estimated from a Luzzati plot. Water molecules were included when the $I2F_oI–IF_cI$ electron density map showed a roughly spherical peak larger than 1 and 3 σ in hydrogen bond distance to a polar atom of the protein or a cofactor.

3. Results

3.1. PSII inhibition assay

Fig. 1 shows the inhibition titration curve of capsaicin in PSII, as measured by the oxygen evolution rates. As indicated, capsaicin inhibits oxygen evolution. In order to determine the dissociation constant for capsaicin on PSII, the inhibition curve was obtained by a non-linear fitting procedure to the equation derived from classical competitive inhibition as following: $f_{Q_B} = Q/(Q + K_m + (K_m/K_i)\cdot I)$, where Q, K_m and I represent the total quinone concentration in the sample, the affinity constant of Q_B, and the total inhibitor concentration, respectively. This fitting leads to a K_I value of 12.6 ± 5 μM.

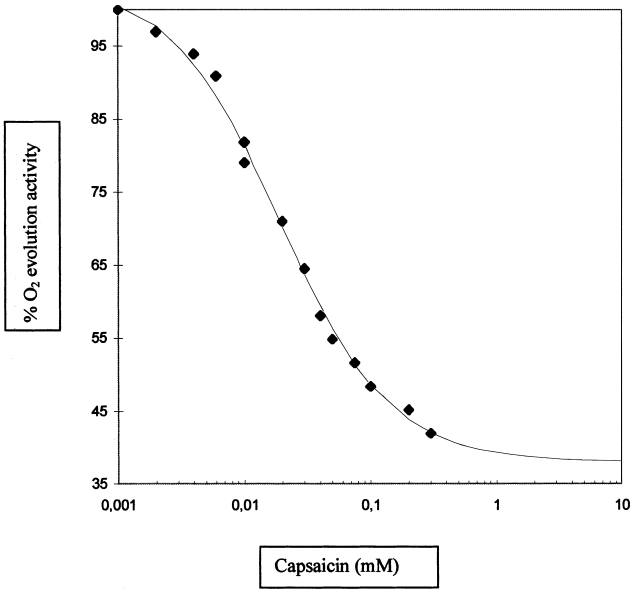

Fig. 1. Effect of capsaicin on oxygen evolution activity of Photosystem II.

3.2. Fluorescence studies

The effect of capsaicin on the fluorescence induction kinetics of PSII (0.4 mg Chl/ml) at pH 7 is presented in Table 1. The ratio F_v/F_m represents the photochemical efficiency of PSII [32]. The F_v/F_m values in the presence and absence of capsaicin, as well as in the presence of 10 μM DCMU, are shown in Table 1.

3.3. Bacterial RC inhibition assay

The inhibitory effect of capsaicin on the RCs from Rb. sphaeroides is seen in the faster decay, which is due to the $P^+ Q_A^- \rightarrow P Q_A$ charge recombination, observed in Fig. 2. Addition of 0.7 mM capsaicin leads to 20% inhibition of the Q_B activity.

Table 1
Effect of DCMU and capsaicin on fluorescence induction kinetics of Photosystem II

	Control	DCMU	Capsaicin
F_v/F_m	0.801	0.590	0.718

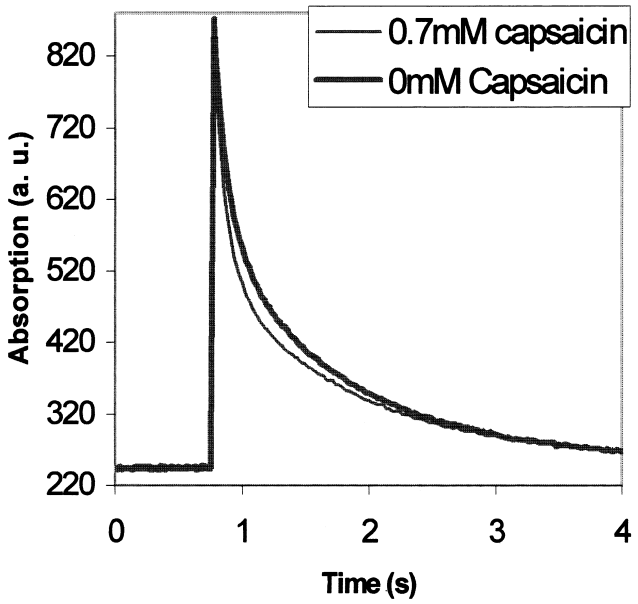

Fig. 2. Charge recombination kinetics. Absorption decay measured at 865 nm following one saturating Yag flash in the absence and in the presence of capsaicin (0.7 mM).

3.4. Crystallographic analysis

The data refinement statistics is listed in Table 2. The $2IF_{obs}I–;IF_{calc}I$ electron density at the Q_B-binding site of a simulated annealing (SA) omit map at a contour level of 1.2 σ, calculated after omission of Q_B is displayed in Fig. 3. The overall shape of the electron density contoured at 1.2 standard deviations (σ) above the mean density correlates well with the dimensions of the capsaicin molecule and not with those of the native ubiquinone (as shown in this figure) and thus allows its placement in the Q_B-pocket. Fig. 4 shows the $2IF_{obs}I–IF_{calc}I$ electron density map at the Q_B-binding site at 1.2 s after inclusion of the capsaicin molecule. The structure of the whole pocket is presented in Fig. 5.

4. Discussion

According to the inhibition titration curve in Fig. 1, capsaicin exhibits a K_I value of 12.6 ± 5 μM in PSII, whereas in the bacterial RC, it behaves as a weak inhibitor. The inhibitory potency of capsaicin on the bacterial RC suggests that the dissociation constant (K_i) of capsaicin is much higher than of other well-known herbicides [33]. The fluorescence induction kinetic studies are also indicative of an electron transfer interruption on the reducing side of PSII in the presence of capsaicin. Our data clearly demonstrate that capsaicin acts as a competitive inhibitor in Photosystem II and the purple bacterial RC. This has interesting implications for the identification of the binding site of capsaicin, especially since capsaicin acts as an inhibitor of the respiratory chain as well. The presence of common inhibitors for multiple quinone reacting enzymes has already been stressed elsewhere [34].

The native quinone, ubiquinone-10 in the wild-type structure based on the trigonal crystal form from *Rb. sphaeroides* [6,7], forms polar interactions through its distal carbonyl oxygen with the peptide nitrogen of Ile L224. In other RC structures (both from *Rp. viridis* and *Rb. sphaeroides*), there is a 5-Å displacement of the position of the Q_B molecule [15].

X-ray crystallographic analysis of the RC with bound capsaicin provided structural details of capsaicin–protein interactions. Even though a significant inhibition of Q_B activity was observed with ubiqui-

Table 2
Data collection and refinement statistics

Beamline	BW6, MPG beam line, DESY Hamburg
Data	
High resolution limit	2.7 Å
No. of measured reflections	151 153
No. of unique reflections (multiplicity)	56 241
Completeness	93.7%
R_{sym}	5.9%
I/σ (outer shell)	2.8
Refinement	
Resolution range	10.0–2.7 Å
R_{free}	23.8%
R_{cryst}	20.3%
Maximum coordinate error	0.34 Å
Average B factor	56.5 Å^2
n_{obs}/n_{par}	1.9
Rms deviations from ideal values	
Bond lengths	0.008 Å
Bond angles	1.05°
Dihedral angles	23.6°
Improper angles	0.34°

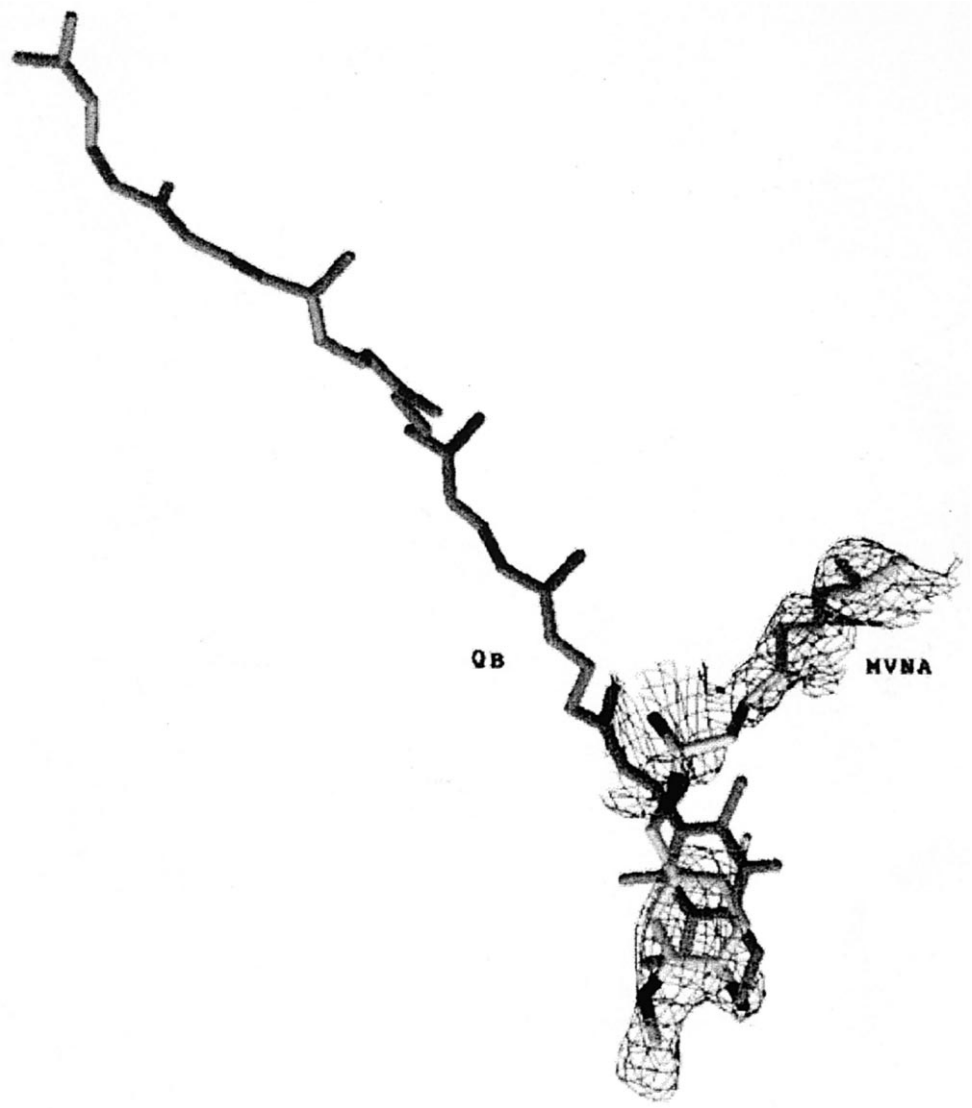

Fig. 3. Simulated annealing omit map at the Q_B site, calculated after omission of the secondary quinone (Q_B) and contoured at 1.2 σ. The capsaicin molecule is shown as a reference. The native quinone (Q_B) is shown for comparison.

none-10 containing RCs, it was important to soak capsaicin with Q_B-depleted RC crystals in order to enhance the capsaicin occupancy in the Q_B pocket. The positions and orientations of the cofactors in this structure are almost identical to the ones in the wild-type structure. The average temperature factor for capsaicin is almost 100 $Å^2$ (75 $Å^2$ for the native quinone in the wild-type structure), whereas the average temperature factor for the whole structure is 56.5 $Å^2$ (34.7 $Å^2$ in wild-type) suggesting that the binding site is only partly occupied.

One binding site for capsaicin is identified, which is located in the Q_B site (Fig. 5). Like the native quinone, capsaicin spans the whole pocket. However, capsaicin is deeper buried in the Q_B-binding site, than Q_B in the wild-type structure from Rb. sphaeroides and the Q_B inhibitors of the triazine class in the *Rp. viridis* RC [16]. The vanilloid group binds at the bottom of the pocket and stacks with Phe L216. The two aromatic rings are nearly parallel to each other and are in van der Waals contact. Capsaicin forms two weak hydrogen bonds with the protein. The capsaicin hydroxyl group can act as a hydrogen donor to the side chain oxygen of serine L223 (about 4.05 Å away), while the capsaicin methoxy oxygen can accept a hydrogen from the peptide amino group of

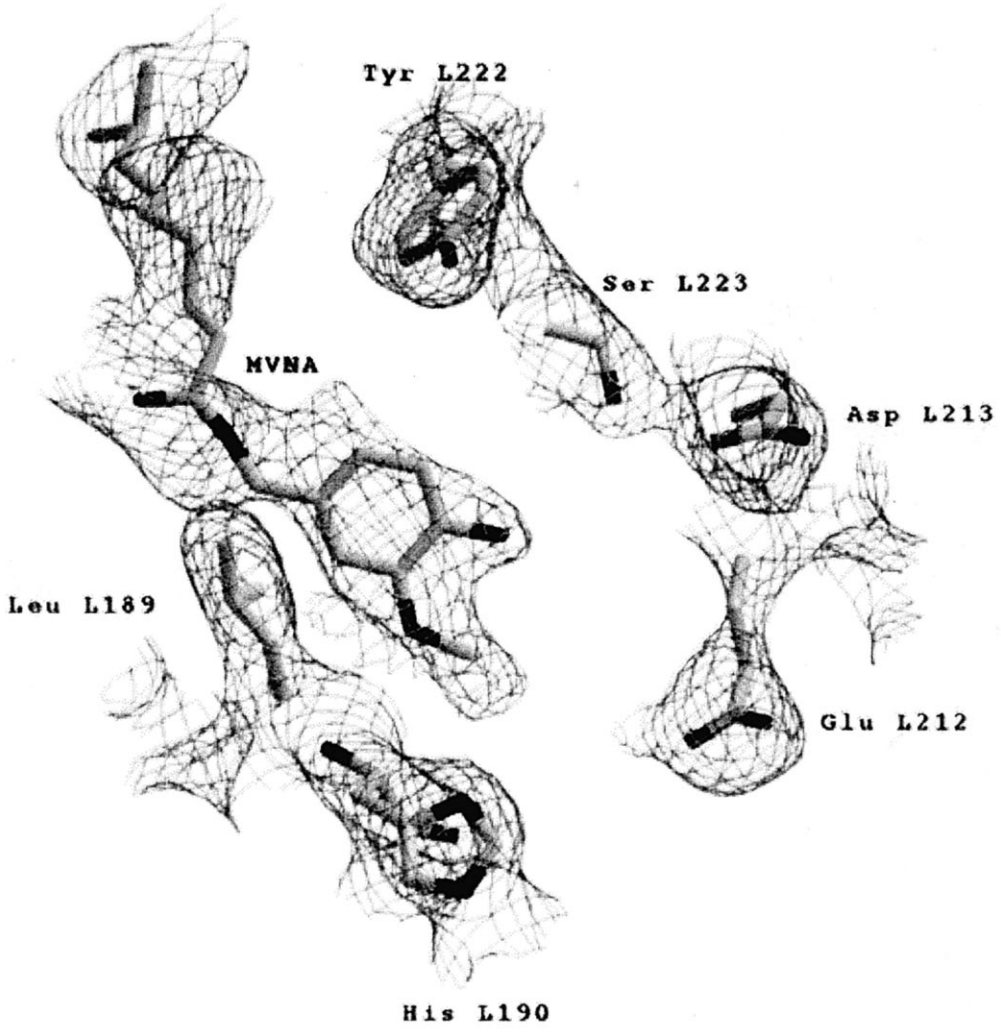

Fig. 4. Simulated annealing map at the Q_B site, calculated after inclusion of the capsaicin molecule and contoured at 1.2 σ.

histidine L190 (about 3.85 Å away). The amide bond group which could serve as a hydrogen-bond donor and acceptor, seems to have no contribution to the binding. However, the hydrophobic chain stabilizes the binding by anchoring to the pocket via hydrophobic interactions. Apparently hydrophobic contacts between the inhibitor and the protein seem to contribute most of the binding energy.

Due to the high homology in the Q_B site between the bacterial RC and PSII, we assume that capsaicin has a similar orientation in the Q_B pocket in PSII, especially since the amino acids (His-190, Ser-223, Phe-216) involved in capsaicin binding in the bacterial RC are found to be conserved in PSII (His-215, Ser-264, Phe-255). However, further studies are necessary in order to clarify the actual binding site for capsaicin in PSII. A series of capsaicin analogs are now being tested in order to examine the structural factors required for the inhibitory action.

Acknowledgements

We acknowledge help in use of the Synchrotron facilities at DESY by the staff of the Max-Planck Research Unit. We would also like to thank Dr. Grabarse for useful discussions and advice on crystallographic refinement and Prof. Kotzambasis for his help with the fluorescence experiments. This work was supported by a grant from the European

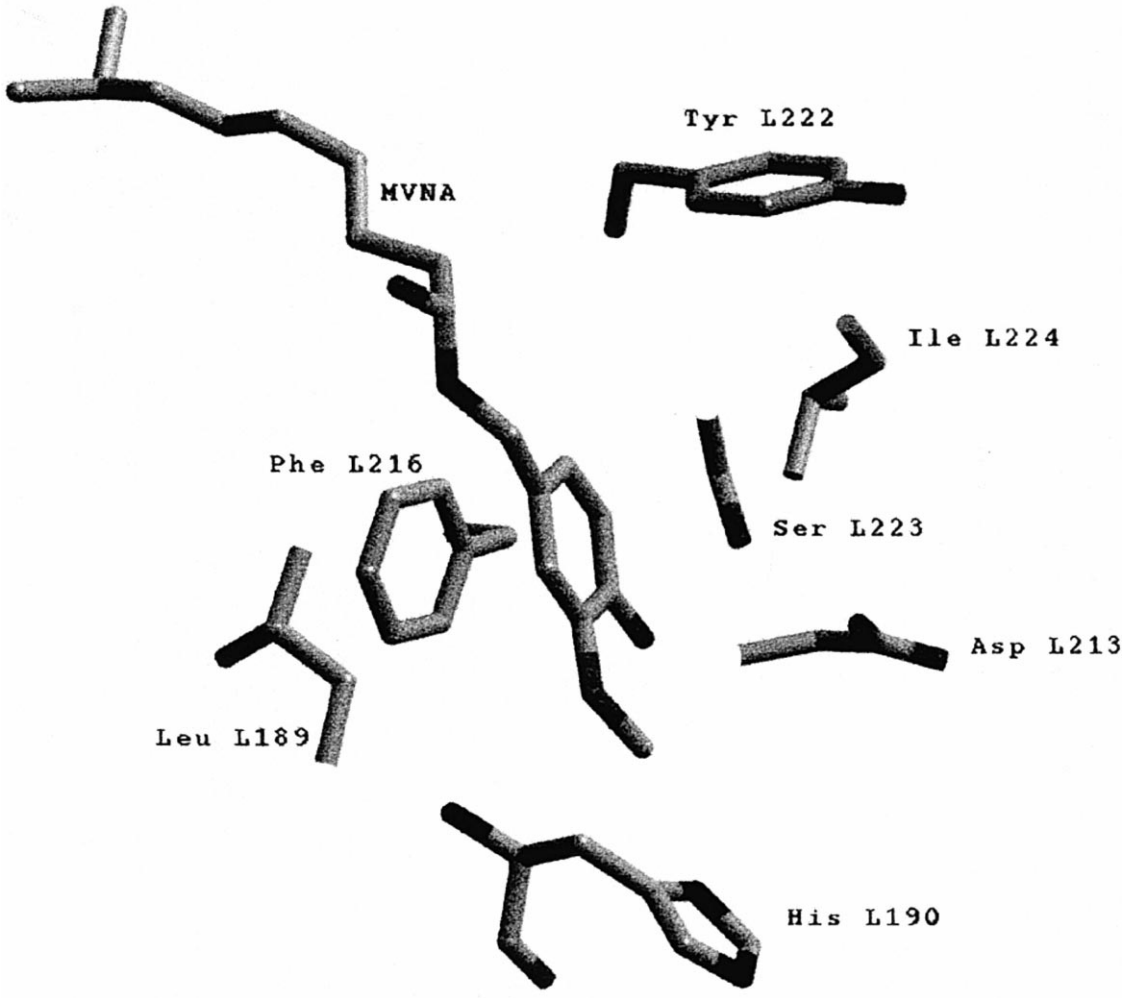

Fig. 5. Overall structure of the Q_B-binding site with capsaicin.

Commission (HC&M: ERBCHRXCT940524) and a grant from the Greek Secretariat of Research and Technology.

References

[1] P. Mathis, Biochim. Biophys. Acta 1018 (1990) 163–167.
[2] R.R. Stein, A.L. Castellvi, J.P. Bogacz, C.A. Wraight, J. Cell. Biochem. 24 (1984) 243–259.
[3] W. Tischer, H. Strotmann, Biochim. Biophys. Acta 460 (1977) 113–125.
[4] J.R. Bower, P. Camilleri, W.F.J. Vermaas, in: N.A. Baker (Ed.), Topics in Photosynthesis, Vol. 10, Herbicides, Elsevier, 1991, pp. 27–85.
[5] M.M.B. Stowell, T.M. McPhillips, D.C. Rees, S.M. Soltis, E. Abresch, G. Feher, Science 276 (1997) 812–816.
[6] E.C. Abresch, M.L. Paddock, M.H.B. Stowell, T.M. McPhillips, H.L. Axelrod, S.M. Soltis, D.C. Rees, M.Y. Okamura, G. Feher, Photosynth. Res. 55 (1998) 119–125.
[7] G. Fritzsch, L. Kampmann, G. Kapaun, H. Michel, Photosynth. Res. 55 (1998) 127–132.
[8] A. Trebst, Z. Naturforsch 41c (1986) 240–245.
[9] S.P. Mackay, P.J. O'Malley, Z. Naturforsch. 48c (1992) 191–198.
[10] A. Trebst, W. Draber, Photosynth. Res. 10 (1986) 381–392.
[11] A. Trebst, Z. Naturforsch. 42c (1987) 742–750.
[12] J. Xiong, S. Subramaniam, Protein Sci. 5 (1996) 2054–2073.
[13] J. Deisenhofer, H. Michel, EMBO J. 8 (1989) 2149–2170.
[14] V. Sobolev, M. Edelman, Proteins 21 (1995) 214–225.
[15] U. Ermler, G. Fritzsch, S.K. Buchanan, H. Michel, Structure 2 (1994) 925–936.
[16] C.R.D. Lancaster, H. Michel, Structure 5 (1997) 1339–1359.
[17] T. Satoh, H. Miyoshi, K. Sakamoto, H. Iwamura, Biochim. Biophys. Acta 1273 (1996) 21–30.
[18] Y. Shimomura, T. Kawada, M. Suzuki, Arch. Biochem. Biophys. 270 (2) (1989) 573–577.
[19] T. Yagi, Arch. Biochem. Biophys. 281 (1990) 305–311.

[20] D.J. Morre, P.-J. Chueh, D.M. Morre, Proc. Natl. Acad. Sci. USA 92 (1995) 1831–1835.
[21] K. Sakamoto, H. Miyoshi, K. Matsushita, M. Nakagawa, J. Ikeda, M. Ohshima, O. Adachi, T. Akagi, H. Iwamura, Eur. J. Biochem. 237 (1996) 128–135.
[22] D.F. Ghanotakis, G.T. Babcock, C.F. Yocum, Biochim. Biophys. Acta 765 (1984) 388–398.
[23] S.K. Buchanan, G. Fritzsch, U. Ermler, H. Michel, J. Mol. Biol. 230 (1993) 1311–1314.
[24] Z. Otwinowski, W. Minor, in: C.W. Carter, R.M. Sweet, (Eds.) Macromolecular Crystallography, Vol. 276, Methods of Enzymology, Academic Press, New York, 1997, pp. 307–326.
[25] D. Gewirth, The HKL Manual, 4th edn., Department of Molecular Biophysics and Biochemistry, Yale University, New Haven, CT, 1995.
[26] G.J. Kleywegth, CCP4/ESF-EACBM Newslett., Protein Crystallogr. 31 (1995) 45–50.
[27] G.J. Kleywegth, CCP4/ESF-EACBM Newslett., Protein Crystallogr. 31 (1996) 45–50.
[28] G.J. Kleywegth, T.A. Jones, in: C.W. Carter, R.M. Sweet (Eds.), Macromolecular Crystallography, Vol. 277, Methods of Enzymology, Academic Press, New York, 1997, pp. 208–230.
[29] T.A. Jones, J.-Y. Zou, S.W. Cowan, M. Kjeldgaard, Acta Crystallogr. A 47 (1991) 110–119.
[30] R.A. Laskowski, M.W. MacArthur, D.S. Moss, J.M. Thornton, J. Appl. Crystallogr. 26 (1993) 283–291.
[31] A.L. Morris, M.W. MacArthur, E.G. Hutchinson, J.M. Thornton, Proteins 12 (1992) 345–364.
[32] B.J. Strasser, R.J. Strasser, in: P. Mathis (Ed.), Photosynthesis: from Light to Biosphere, Vol. V, Kluwer Academic, Dordrecht, 1995, pp. 977–980.
[33] L. Baciou, E.J. Bylina, P. Sebban, Biophys. J. 65 (1993) 652–660.
[34] M.D. Esposti, A. Ghelli, M. Crimi, E. Estorneli, R. Fato, G. Lenaz, Biochem. Biophys. Res. Commun. 3 (1993) 1090–1096.